8th IAA Planetary Defense Conference – PDC 2023

3-7 April 2023, Vienna, Austria

IAA - PDC 23-04-06
Vienna, Austria

TOPIC: Impact Effects & Consequences

COMPUTATIONAL ANALYSIS OF GROUND EFFECTS FROM BOLIDE DISRUPTION VIA THE PI METHOD

Dharv Patel [1], Brin Bailey [1], and Philip Lubin [1]

[1]Department of Physics, University of California – Santa Barbara, Santa Barbara, CA 93106, USA, (805) 893-8432, (dharv@ucsb.edu, brittanybailey@ucsb.edu, lubin@ucsb.edu, ancohen@ucsb.edu)

Keywords: Planetary Defense, Atmospheric Airbursts, Simulations

ABSTRACT

The PI ("Pulverize It") method proposed by Lubin et. al. is a method for planetary defense from asteroids and comets which can operate in a terminal interdiction mode with extremely short warning times. The PI method mitigates an incoming threat by completely disrupting the bolide via hypervelocity penetrators, producing a fragment cloud with lateral, longitudinal and temporal spread which enters Earth's atmosphere and results in a series of airburst events at varying altitudes >30 km. This highly de-correlates and distributes the energy of the original parent bolide, as the burst times of the individual fragments are separated by times that are longer than the blast wave pulse duration for each airburst. Although de-correlated, each airburst produces ground effects which are important to analyze to design mission profiles with acceptably low damage. The primary ground effects of concern include optical flashes, acoustical blast waves, wind effects, and dust production. Using a Monte Carlo simulation technique which models the airburst events from a specified number of fragments, we explore a variety of cases with varying intercept times and disruption energies and find that threats mitigated by the PI method produce vastly less damage on the ground when compared to the same unfragmented case. Our model follows each fragment resulting from the disruption of the parent bolide and computes the resulting acoustic blast wave and optical signature produced by it for any observer on the Earth. The model inputs the parent bolide diameter, speed, density distribution, angle of attack, yield strength and fragmentation distribution, and allows for statistical variations in the fragmentation process, which in turn leads to variation in the time evolution of the resulting acoustic and optical signatures at the surface of the Earth. We show that for an 800m diameter threat with >10 years of warning time, the PI method offers an effective planetary defense solution that makes use of pre-existing technologies and launch vehicles. We show that the ground effects from an 800m bolide fragmented into <10m pieces are reduced to short- and long-term non-lethal effects by intercepting the threat as little as 100 days prior to impact, and that further reduction of the ground effects can be achieved with far earlier intercept times. In this scenario, most of the fragments miss Earth entirely and those that do impact Earth are <10m in diameter and are highly de-correlated, leading to blast wave over-pressures well under 2kPa and optical energy distribution of no greater than 10kJ/m^2. Our simulations show that PI can mount a realistic terminal defense mission profile for an 800m asteroid with an intercept time as

low as 75 days.

1. Background

Impact threat

Throughout the past several decades, collisions of Near-Earth Objects (NEOs) with Earth have captured both scientific and public attention. Though the majority of incoming bolides intercept Earth with low impact energies (Fig. 1), asteroid and comet impacts pose a continual threat to humanity. Historical events such as the Chelyabinsk asteroid impact in 2013 (released energy equivalent to 570 ±150kt TNT) and the Tunguska event in 1908 (air blast energy yield of 3-30Mt) have served as reminders that Earth is not impenetrable to such threats [1], [2]. Objects at least the size of the Chelyabinsk asteroid (~20m diam.) are expected to impact Earth approximately every 50-100 years, while objects with the energy of the Tunguska threat (estimated ~65m diam.) are expected to impact Earth approximately every 800-1800 years [2].

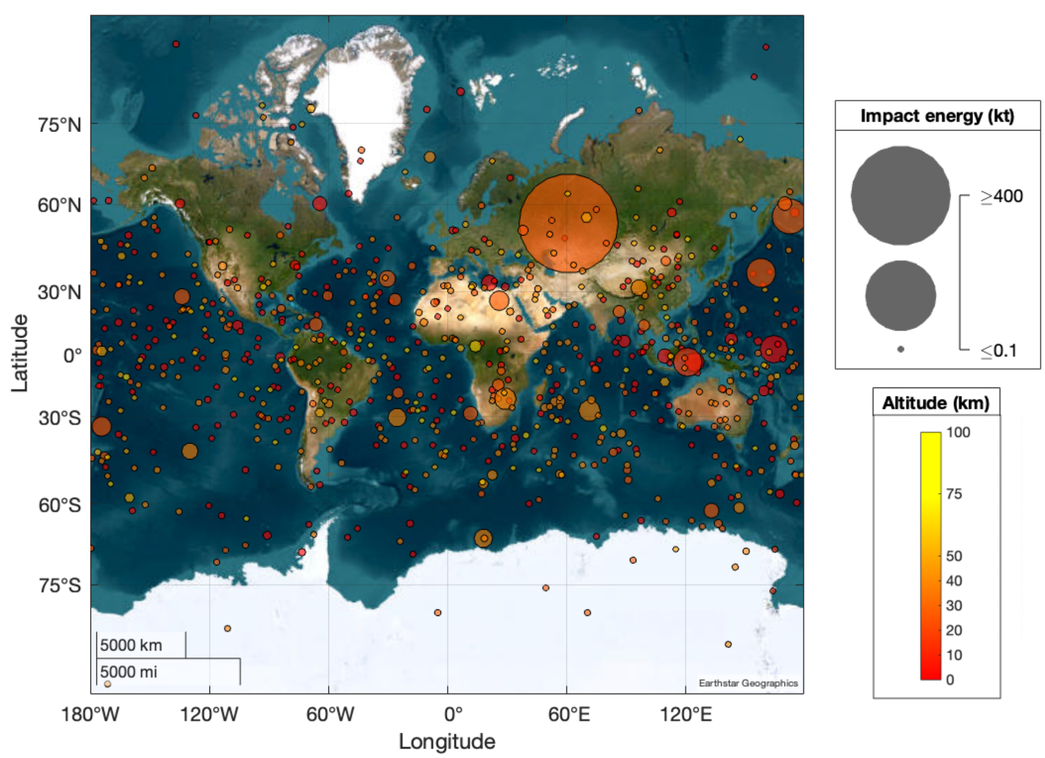

Figure 1. Map of airburst impacts from atmospheric infrasonic sensors. Data span 757 events greater than 0.073kt from April 15, 1988 through Sept 29, 2021. The largest bubble, seen over Russia, displays the 2013 Chelyabinsk event. Data from Alan B. Chamberlin (JPL/Caltech) https://cneos.jpl.nasa.gov/fireballs/.

While impacts of objects of <100m diam. are much more likely than larger threats (≥100m diam.), larger objects maintain the possibility of posing a great threat to human life. The near-Earth asteroid 99942 Apophis, a potentially hazardous asteroid (PHA)

with a diameter of 340m, will make its next closest approach to Earth on April 13, 2029, where it will approach within Earth's geosynchronous orbit. A PHA of this size encountering Earth this closely is expected to occur approximately every 1000 years [3]. For reference, Apophis is 7 times larger and 350 times more massive than the Tunguska 1908 impactor [4], while 5000 times more massive than the Chelyabinsk 2013 asteroid [1]. If Apophis were to collide with Earth, it would have an impact yield of approximately 3-4Gt TNT equivalent [2], equal to about half of Earth's total nuclear arsenal. Continuous observations of Apophis since its discovery in 2004 have almost entirely ruled out the possibility of an impact occurring in 2029, though the possibility of collision during a resonant return of Apophis to Earth is non-zero [5]. Larger than Apophis is asteroid 101955 Bennu with a diameter of about 500m, whose impact could pose a yield of approximately 10Gt TNT equivalent [2], greater than that of Earth's total nuclear arsenal. Objects even larger have the potential to enact cataclysmic, large-scale effects on humanity and Earth as a whole if an impact were to occur.
While these objects currently post no threat to Earth, it is conceivable that objects of their sizes could impact Earth in the future. Effective mitigation strategies are imperative to the prevention of harm to human life.

Mitigation strategies

Several different methods of mitigation have been proposed for planetary defense. The method most commonly cited is deflection via kinetic impact, in which a spacecraft would intercept a threat to modify the object's orbit through momentum transfer. In 2022, NASA conducted the first full-scale demonstration of asteroid deflection technology with the Double Asteroid Redirection Test (DART) to test deflection as an effective mitigation strategy. DART successfully deflected the near-Earth asteroid 65803 Didymos and altered its orbital time by 32 $\pm$2 minutes.
The drawback to deflection as an effective mitigation strategy is that, in order to successfully launch a mission to intercept a threat at a proper distance , the orbital path of the object must be accurately observed–and thus predictable–decades or longer before a potential impact. This poses a challenge, as the orbital evolution of an asteroid is affected by a host of physical properties (albedo, size, shape, rotation, physical structure, thermal properties) that may be difficult to measure accurately [6]. The lack of availability of such properties can become a limiting factor that leads to uncertainties in the role played by non-gravitational effects on that orbit [6]. Without several years of accurate observation of an incoming threat and total preparedness of a launch mission (mission planning, appropriately sized kinetic impactor spacecraft and launch vehicle, etc.), deflection may become an ineffective mitigation strategy for short timescales.
We propose a mitigation strategy described by Lubin and Cohen [7] by which a more offensive approach is taken. The PI ("Pulverize It") method involves an array of small hypervelocity kinetic penetrators that pulverize and disassemble an asteroid or small comet into small (maximum ~10m diam.) fragments, producing a fragment cloud with spatial and temporal spread. PI is a practical and effective method for planetary defense which can operate in a terminal interdiction mode with extremely short warning times. Compared to other threat reduction scenarios, this approach requires much less launch mass and represents an extremely rapid response, testable method, and deployable approach using existing technologies.

2. Methods

Intercept scenarios

The proposed system is an effective mitigation strategy for planetary defense that will work in extended time scale interdiction modes where there is a large warning time, as well as extremely short interdiction time scales with intercepts of days to even minutes before impact. PI allows for effective defense against bolides in the 20-1000m diameter class and could virtually eliminate the threat posed by an impact of such objects, though the effectiveness of the approach depends on the time scale of interception as well as the size, composition and speed of the bolide. In longer intercept scenarios, the resultant fragment cloud largely or entirely misses Earth. Such a scenario is, of course, preferable; however, we show that short intercept scenarios work to effectively distribute the energy of the parent bolide such that the yield is decreased in comparison to the unfragmented threat. In shorter intercept scenarios, the fragment cloud enters Earth's atmosphere, where the fragments of maximum ~10m diameter burn up and/or airburst at varying altitudes >30km. The primary channel of energy is diverted into spatially and temporally de-correlated shock waves, effectively distributing the energy of the original parent bolide as the burst times of the individual fragments are separated by times that are longer than the blast wave pulse duration for each airburst.

This approach allows for terminal defense in the event of short warning time and short target distance mitigation where orbital deflection is not feasible. Lubin [8] describes five basic modes of operation of the method which depend on a combination of warning time and threat magnitude. The product of the intercept time τ_{impact} (the time at which the threat is intercepted relative to its impact time) and the disruption speed v_{dis} is the main metric on which these mitigation modes are based. Larger disruption speed allows for shorter intercept time such that $\tau_{impact} \sim 1/v_{dis}$. In general, we assume a very conservative v_{dis}= 1m/s in calculating the intercept times for all cases unless otherwise indicated. This study assumes stony densities (~2.6g/cc) for our threat analysis, though a wider range of densities and cohesive strengths are explored in Lubin [8]. A summary of the first three of five basic modes of operation, taken from Lubin [8], can be seen below. We omit modes (4) and (5) here as they describe existential threats (1km diam. and above) which are not pertinent to this exercise.

1) Short time warning (terminal defense) – minutes to days intercept (15-100m diam. threats)
    - Threat is disassembled into fragments of <15m diam. that enter and burn up in Earth's atmosphere
    - Fragment cloud is fairly concentrated
    - Shock waves de-correlated – virtually no damage, though possible minor window damage
    - Sum of all optical pulses below combustion limit – no fires
    - Ex: 100m diam. (~100Mt >> Tunguska) can be mitigated with 1 day intercept
    - Ex: 20m (0.5Mt – Chelyabinsk) can be mitigated with 100 sec intercept (10m/s disruption)

2) Moderate time warning – 10-60 day intercept (100-500m threats)
    - Threat is disassembled into fragments of <15m diam. that enter and may burn up in Earth's atmosphere
    - Fragment cloud spreads over large area on Earth (~1000km radius)
    - Ex: 350m diam. (~4Gt – Apophis) can be mitigated with 10 day intercept
    - Ex: 500m diam. (~8Gt – Bennu) can be mitigated with 20 day intercept
3) Longer time warning – >75 day intercept (600-1000m threats)
    - Threat is disassembled into fragments of ideally <15m diam., but less restrictive
    - Fragment cloud spreads to be larger than Earth
    - Virtually all fragments miss Earth
        - Residual fragments <15m diam. that may hit the Earth are not a threat; mitigated by atmosphere
        - Residual fragments >15m diam. may be mitigated using mode (1) if necessary

A more thorough explanation of the overall PI system, including comprehensive explanations and detailed descriptions of methods and examples, can be found in Lubin and Cohen [7] and Lubin [8].

Acoustical ground effects

The acoustical ground effects from an asteroid burst can be related to and approximated by those of nuclear blasts as discussed in Boslough [11]. Due to this reason, we simulate the acoustical ground effects from mitigation via the PI method from measurements of equivalent nuclear blasts. To model the time evolution of the shock wave, we use a Friedlander functional form [Eq. 1]. This describes the time evolution with two free parameters which are the peak pressure (P_0) and a zero crossing time scale (t_0). This also allows us to compute the time evolution of the acoustical pressure and flux. The time t=0 is when the shock wave first arrives at the observer, not to be confused with the time at which the fragment bursts.

$$P = P_0 \cdot e^{-t/t_0}(1 - t/t_0) \quad (1)$$

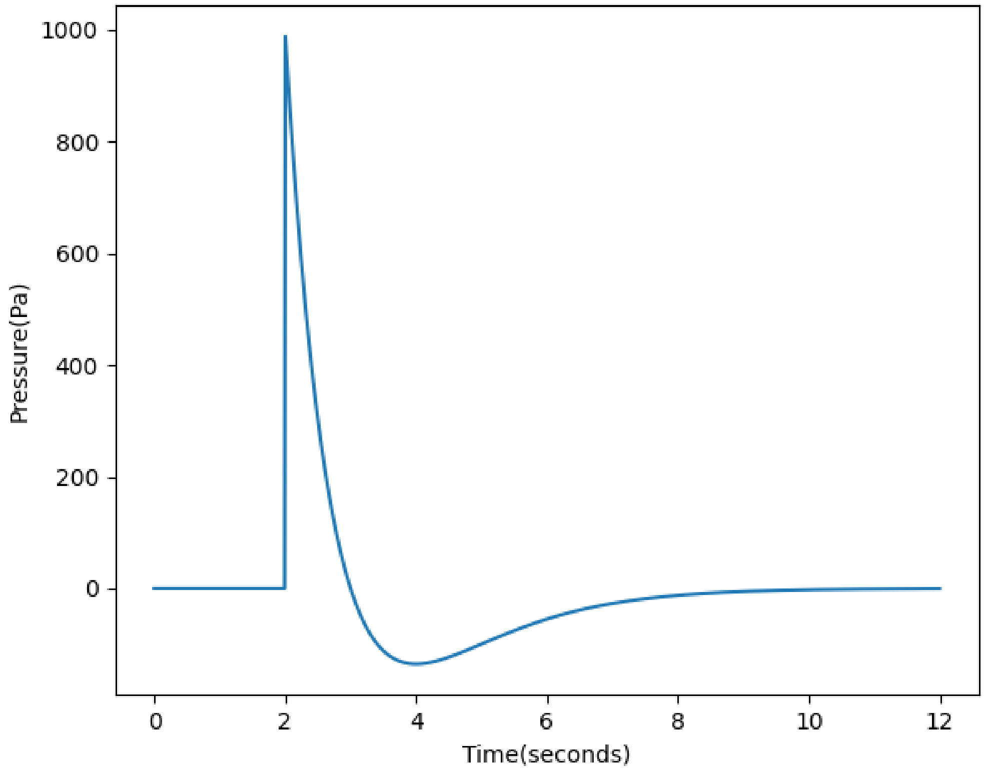

Figure 2. Example of the Friedlander equation applied to a single blast wave with an overpressure of 1 kPa. Time decay number is 1s.

The peak pressure for an asteroid that has energy (in kt) of E_{ast-kt} in the blast wave is calculated from the equivalent energy of a nuclear weapon with $E_{nuc} = E_{ast-kt}/\epsilon$ as

$$P_0 = p_n\left[r(E_{ast-kt}/\epsilon)^{-1/3}\right]^{\alpha_n} + p_f\left[r(E_{ast-kt}/\epsilon)^{-1/3}\right]^{\alpha_f} \quad (2)$$

where r is the distance to burst, and p_n, α_n, p_f, α_f are near and far effects of the equivalent blast, respectively. We then simulate the bursts using [Eq. 1] and [Eq. 2] and add their effects to simulate any constructive/destructive interference. One key input required after this is the t_0 parameter used in the Friedlander Equation. We calculate this parameter using the relation to pressure, meaning the width of the Friedlander wave changes based on the energy being deposited into the region. This is a direct result of the extrapolation done by Lubin [8] based on data by Brode [10]. This is shown in [Eq. 3] where p is the pressure at that point. We conducted simulations using a Monte-Carlo method to test our data and found that simulations are reasonably equivalent with the rough estimates of overpressure from recorded events such as Chelyabinsk.

$$t_0 = \begin{cases} -0.07755 \cdot \ln(p) + 1.051 & \text{for p} < 200\text{kPa} \\ 0.01246 \cdot \ln(p) - 0.07758 & \text{for p} > 200\text{kPa} \end{cases} \quad (3)$$

Optical ground effects

Optical pulses result following disassembly as the small asteroid fragments burn up in Earth's atmosphere. Large optical pulses, possibly resulting from either an unmitigated impact or an extremely short time scale interception with large numbers and/or sizes of fragments, may cause harm in several ways. These include but are not limited to: skin damage (sunburn) due to bursts occurring below the ozone layer; optical (eye) damage due to high power flux and little to no atmospheric protection; and fire (beginning at an energy flux of 200kJ/m^2). To simulate the electromagnetic output of one of these bursts, we approximate the asteroid as a blackbody source and use a Gaussian power distribution to describe how the energy flux changes with interception. To construct the Gaussian wave, we first take the total energy of the asteroid and convert approximately 10% of it into E-M radiation. This number depends on the energy in the fragments but approximately comes out to 10-20% on fragments of our size (maximum ~10m diam.). This conversion is an analytical extrapolation from Lubin [8] based on data from Glasstone and Dolan [9], shown in [Eq. 4] where x is the exo-atmospheric energy and E is the energy that goes into optical flux.

$$E = (x/8.2508)^{1.13} \tag{4}$$

We then construct an expression for the power flux using the Gaussian integral equation [Eq. 5] and assume that over the period of the wave, the integral results in this energy flux.

$$\int_{-\infty}^{\infty} e^{-t/2} dt = \sqrt{2/\pi} \tag{5}$$

We propagate this energy flux to each and every observer using the distance propagation of light:

$$E_{obs} = \frac{E}{4\,\pi r} \tag{6}$$

We construct a temporal distribution for the power flux by dividing the E-M energy by √2π. This gives us an expression for power as

$$P = E_{obs} \cdot e^{-t^2} \tag{7}$$

where E_{obs} is the energy flux received by an observer at any point on the grid. We then account for atmospheric absorption. We estimate that the atmospheric transmission is described by

$$T = be^{-ar} \tag{8}$$

where b and a are determined from the atmospheric model fit to the blackbody data and r is the distance to the burst in meters. In our case, we find that b = 1.02 and a = 0.009. This is only valid for larger distances and should not be used as a shorthand for dealing with atmospheric absorption of light on shorter distances. We utilize this approximation as the airbursts from the PI method occur 30-45km above Earth's surface.

When calculating the power, we first calculate the energy flux (E_{obs} in Eq. 6), then input it at time=burst time to simulate an addition of energy flux instantaneously which would be the case with optical effects since the speed of light can be approximated as infinity for our simulations.

Wind and dust production

The effects of wind and dust production following asteroid disassembly via the PI method will be more thoroughly simulated and described in future studies.. Upon burning up, the asteroid fragments are dispersed into many particles that become distributed throughout the atmosphere. We simulate the asteroid distributes its mass into small dust particles of ~1μm diameter as a conservative estimate. We present this estimate as a worst-case scenario, as any smaller diameter would not block light perfectly. Conservatively, this means that the particles would block sunlight and have the potential to cause global atmospheric, and perhaps climatic, effects. We can estimate the amount of surface area covered and simulate the resulting effects as discussed in Lubin [8]. Our calculations show that disassembly of an 800m asteroid into a fragment cloud will yield a particle distribution that covers just under 100% of the surface of the Earth. However, such a scenario would require perfect distribution of the particles, which is not realistic. Realistically, the Hadley cycle combined with the Coriolis effect, resulting in the North-East and South-East Trade Winds, [Fig. 4] would likely influence particle distribution. Additionally, the distribution would rely heavily on the arrangement of dust grain sizes. This is something we are in the process of modeling and will be discussed in future studies.

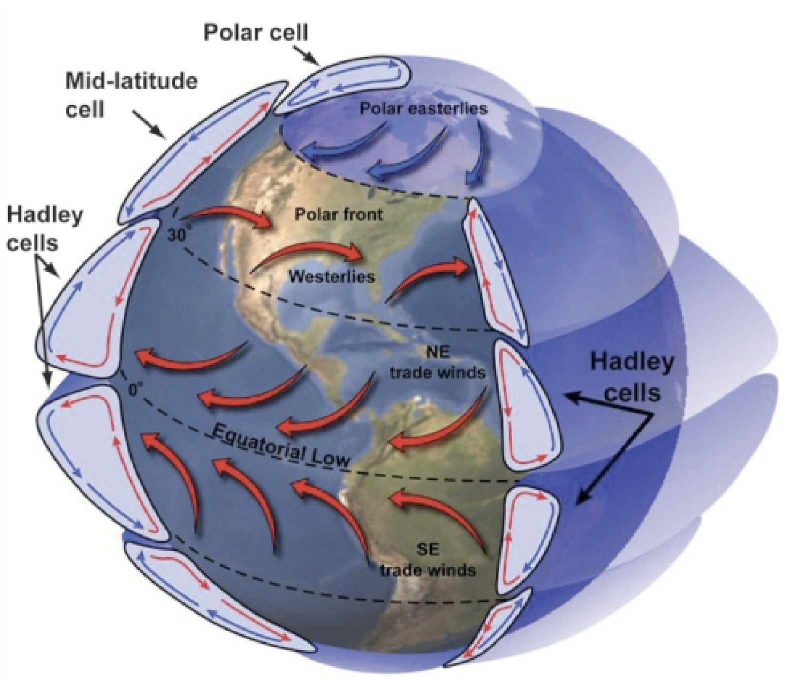

Figure 3. Effects of the Hadley cycle and the Coriolis effect on the creation of the North-East and South-East Trade Winds, taken from Tziperman [12].

3. 2023 PDC

Intercept scenarios

We outline an approach to mitigation of a hypothetical impact of asteroid 2023 PDC via the PI method. Given the initial (April 2023) diameter estimate of 220-660m and 1% impact probability in October 2036, an intercept mission designed for the worst-case scenario (≥660m diam.) could be prepared, and possibly launched, before the size of the asteroid is completely determined. For asteroids with diameters between this estimated range and outside of it (assuming a worst-case scenario up to ~125% of the maximum diameter estimate), our simulations show that the PI method can effectively mitigate such threats with intercept times ranging from days to months.

However, given the warning time of ~13 years prior to impact and the short timescale capability of the preparation for and use of the PI method, the option would exist to defer a launch until adequate observations have been made to narrow down the most likely size range of the asteroid if such a scenario is desired. Such a scenario would allow for more frequent observations, and thus more accurate estimates, of the asteroid's physical properties and orbital path, increasing the accuracy of both a possible interception and probability of a successful mitigation. Assuming this scenario is desired, we then wait for more observations to be made over the following months.

It is then found in July 2024 through more accurate observations of absolute magnitude, albedo and color data that 2023 PDC is likely (52%) to be a C-type asteroid with a diameter likely within 300-880m. Observations have determined an impact probability of 100% yielding an impact energy of approximately 76Mt-10Gt.

We show the results of four different threat cases mitigated by the PI method to describe possible mitigation routes of 2023 PDC. The cases presented vary in size, intercept time, and number of fragments. The various asteroid diameters span the size range of the initial and secondary 2023 PDC diameter estimates, simulating mitigation of 200m, 350m, 500m, and 800m asteroids. The intercept time varies with each size, increasing with asteroid diameter. Each case assumes a stony asteroid (density of 2.6g/cc) traveling at 20km/s (relative to Earth's reference frame) with an angle of attack of 45° and disruption of 1m/s.

Acoustical ground effects

- The acoustical effects are easy to see in the Maximum Hold pressure plot on the right shows the overpressures that happen due to a single burst. Some of our other movies with smaller range in x and y direction shows better temporal evolution in the left plot. It can be found on our youtube channel. The link is provided at the end.

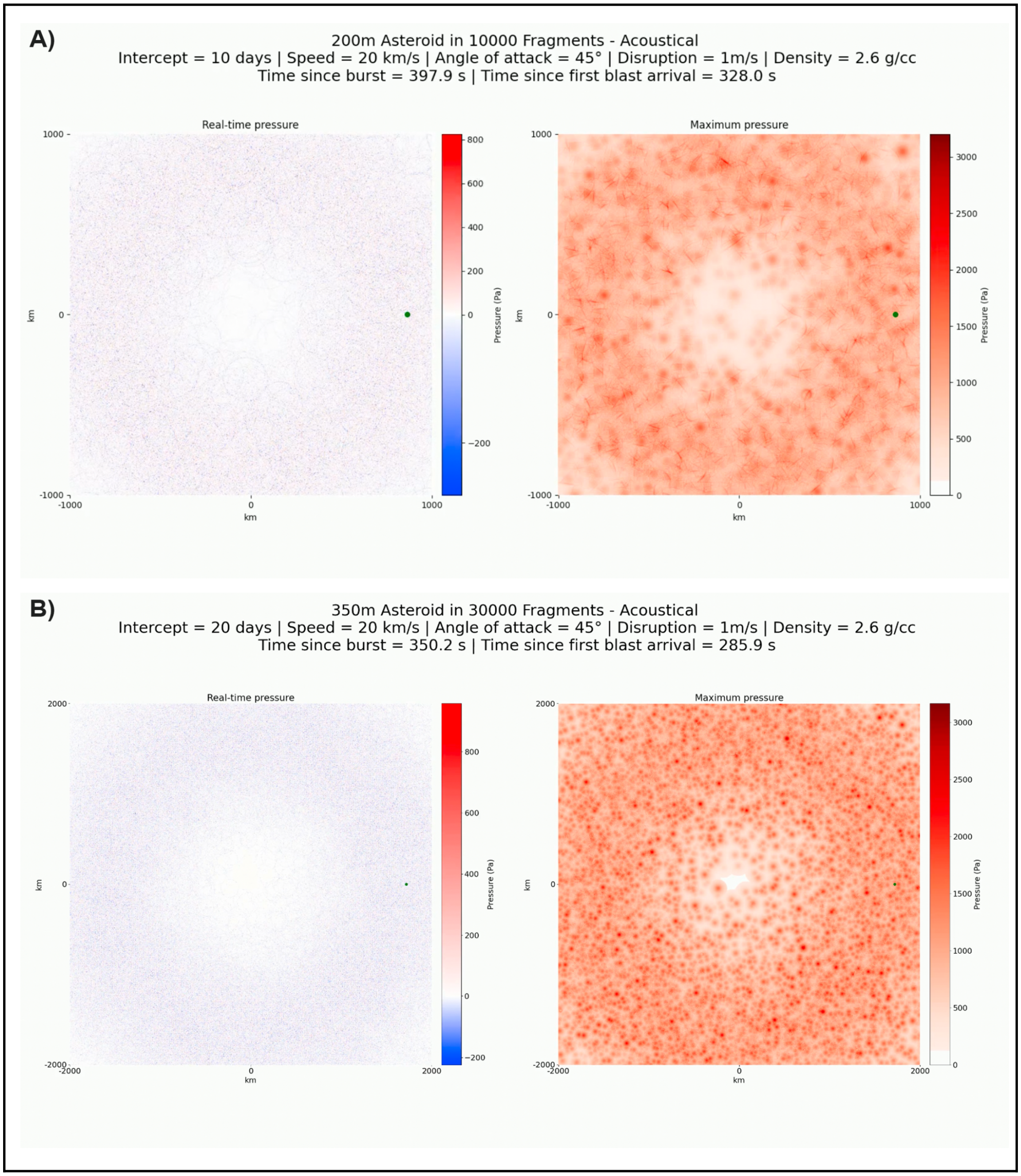
A)
200m Asteroid in 10000 Fragments - Acoustical
Intercept = 10 days | Speed = 20 km/s | Angle of attack = 45° | Disruption = 1m/s | Density = 2.6 g/cc
Time since burst = 397.9 s | Time since first blast arrival = 328.0 s
Real-time pressure
Maximum pressure
Pressure (Pa)
km
B)
350m Asteroid in 30000 Fragments - Acoustical
Intercept = 20 days | Speed = 20 km/s | Angle of attack = 45° | Disruption = 1m/s | Density = 2.6 g/cc
Time since burst = 350.2 s | Time since first blast arrival = 285.9 s
Real-time pressure
Maximum pressure
Pressure (Pa)
km

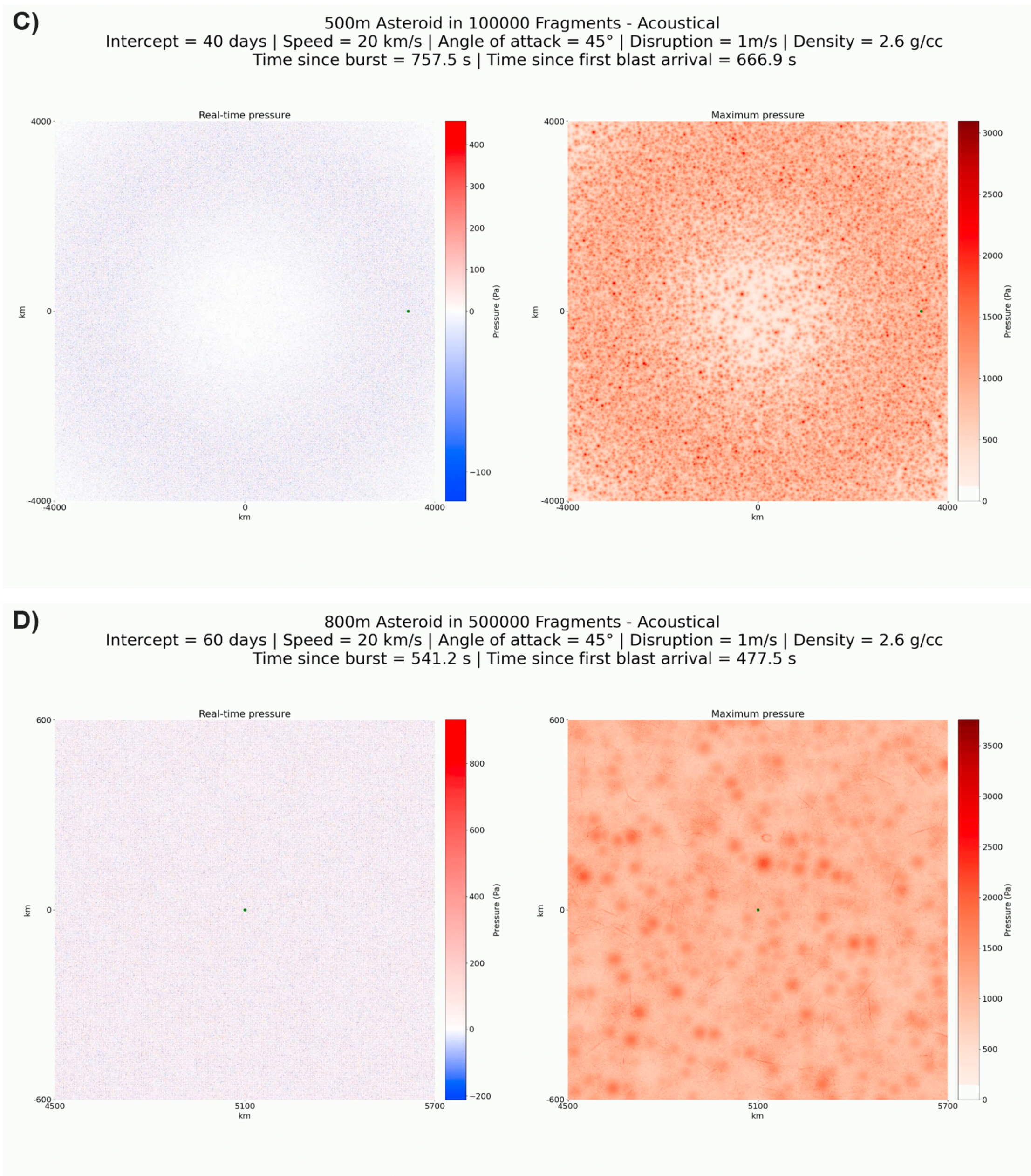

Figure 4. Acoustical blast wave simulations showing mitigation of various potential threats from 200m-800m. The left plot shows the real-time pressure throughout the area; the real-time of each simulation is seen in the title as "Time since burst" (units of sec), dictating the amount of time that has passed since the first airburst of the first fragment. The right plot shows the maximum pressure experienced by each pixel throughout the current length of the simulation. Throughout all simulations, several parameters of the asteroid are held constant: velocity = 20km/s; angle of attack = 45°; disruption velocity = 1m/s; and density = 2.6g/cc. Note that the areas spanned by each simulation (units of km) may differ. **A.** 200m diam. asteroid broken into 10000 fragments with a 10 day intercept. **B.** 350m diam. Asteroid (~Apophis) broken into 30000 fragments with a 20 day intercept. **C.** 500m diam. asteroid (~Bennu) broken into 100000 fragments with a 40 day intercept. **D.** 800m diam. asteroid (~2023 PDC worst-case) broken into 500000 fragments with a 60 day intercept.

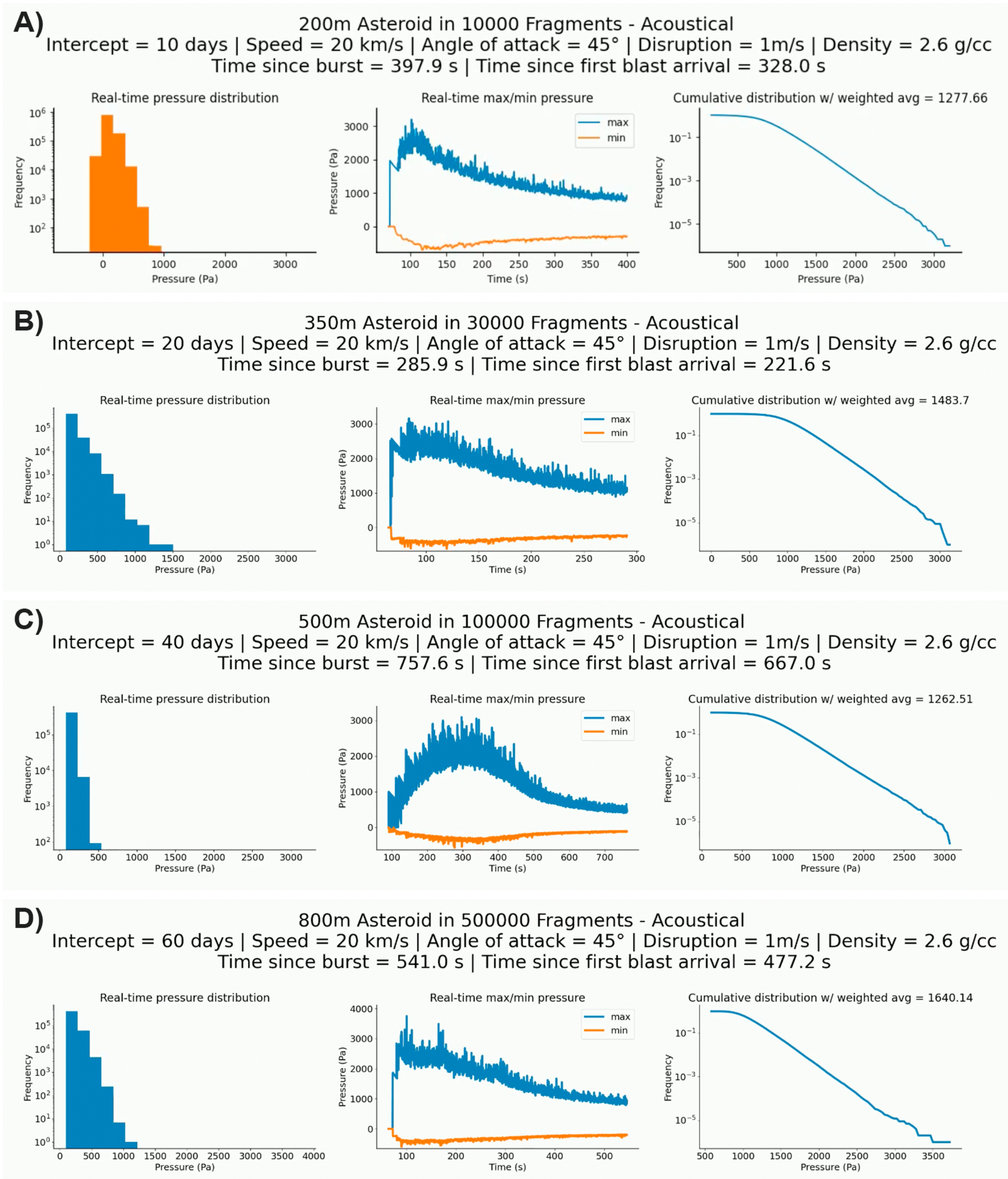

Figure 5. Statistical plots of acoustical blast wave simulations showing mitigation of various potential threats from 200m-800m. Note that each set of plots (A-D) matches the threat cases shown in Figure 4. The left plot shows a histogram distribution of the real-time pressure throughout the area; the real-time of each simulation is seen in the title as "Time since burst" (units of sec), dictating the amount of time that has passed since the first airburst of the first fragment. The middle plot shows the real-time maximum (blue) and minimum (orange) pressures throughout the area. The right plot shows the cumulative distribution function (CDF) dictating the frequency of occurrence of various pressure values. Note that the majority of all airbursts are relatively low in pressure, and high pressure values occur rarely as results of two-point and three-point caustics.

Optical ground effects

- The Optical effects are shown in the figure 6. The Energy Flux is shown on the right and Power flux is on the left. The circular patterns seen are a direct result of the $1/4\pi r^2$ factor where r is the distance from the burst to the observer. .

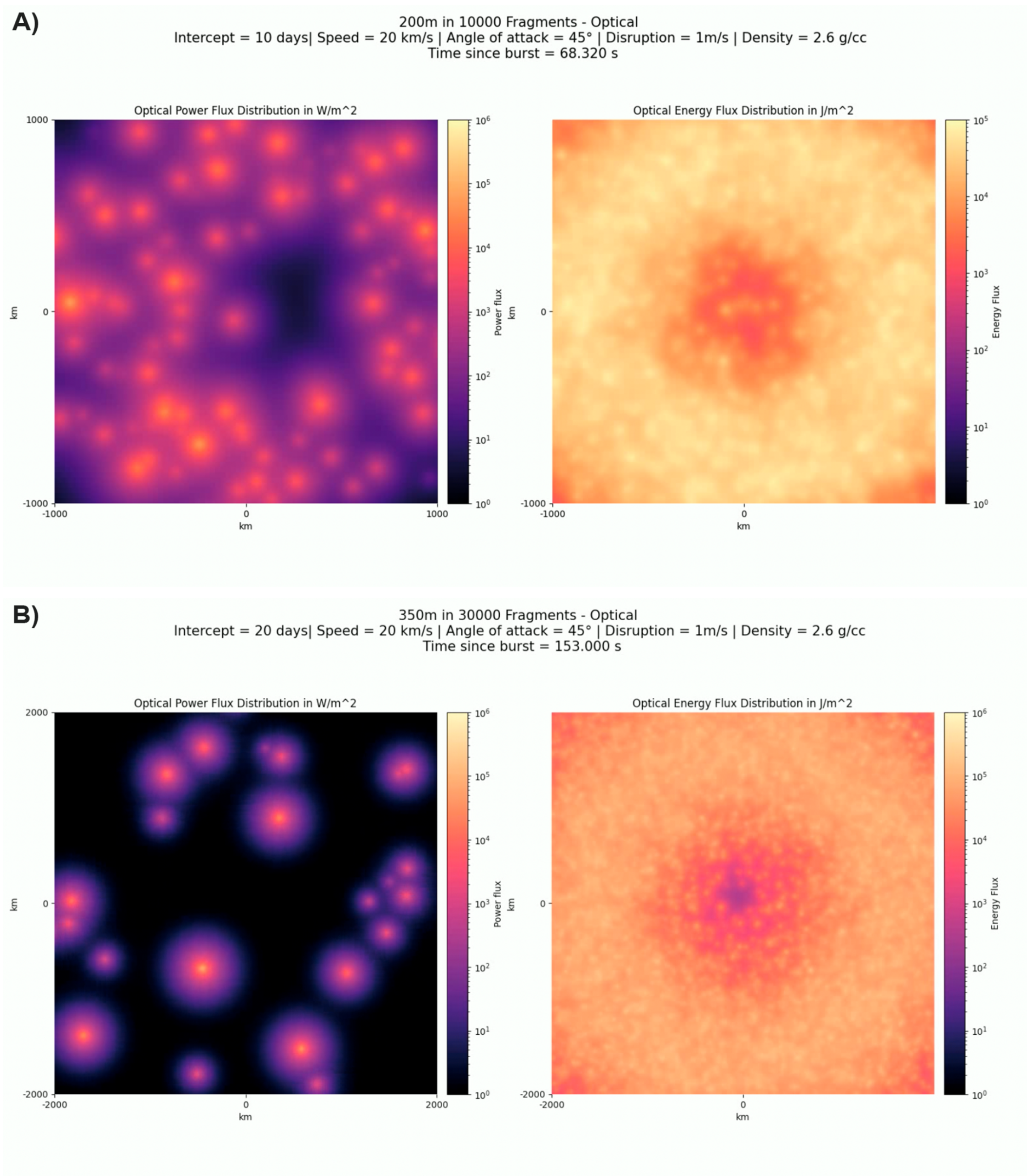

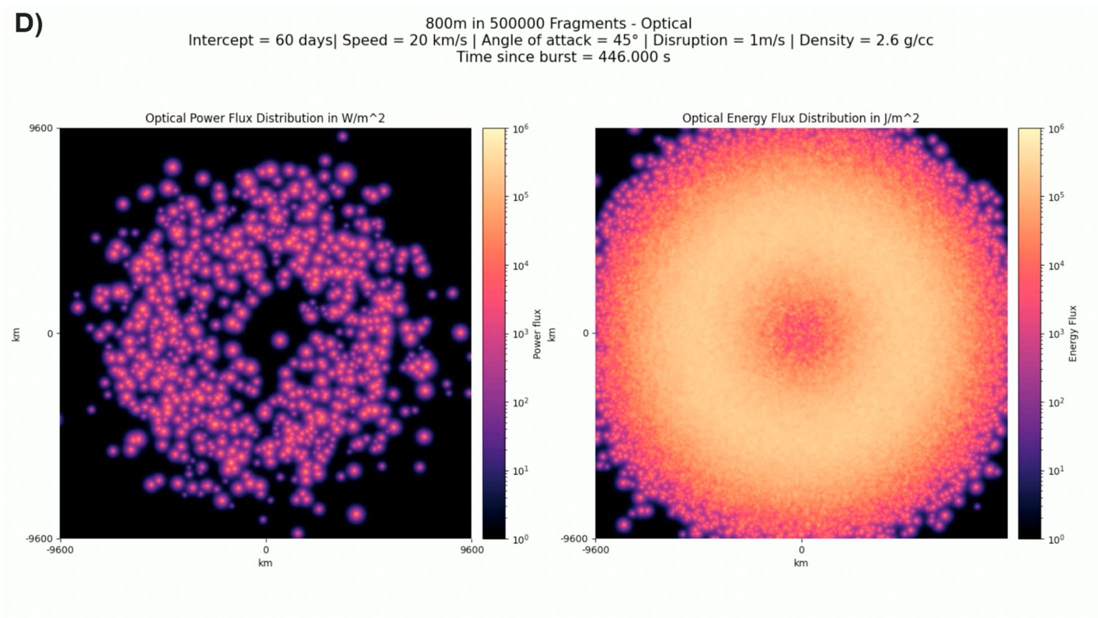

Figure 6. Optical pulse simulations showing mitigation of various potential threats from 200m-800m. The left plot shows the real-time optical power flux throughout the area; the real-time of each simulation is seen in the title as "Time since burst" (units of sec), dictating the amount of time that has passed since the first airburst of the first fragment. The right plot shows the optical energy flux experienced by each pixel throughout the current length of the simulation. Throughout all simulations, several parameters of the asteroid are held constant: velocity = 20km/s; angle of attack = 45°; disruption velocity = 1m/s; and density = 2.6g/cc. Note that the areas spanned by each simulation (units of km) may differ. **A.** 200m diam. asteroid broken into 10000 fragments with a 10 day intercept. **B.** 350m diam. Asteroid (~Apophis) broken into 30000 fragments with a 20 day intercept. **D.** 800m diam. asteroid (~2023 PDC worst-case) broken into 500000 fragments with a 60 day intercept.

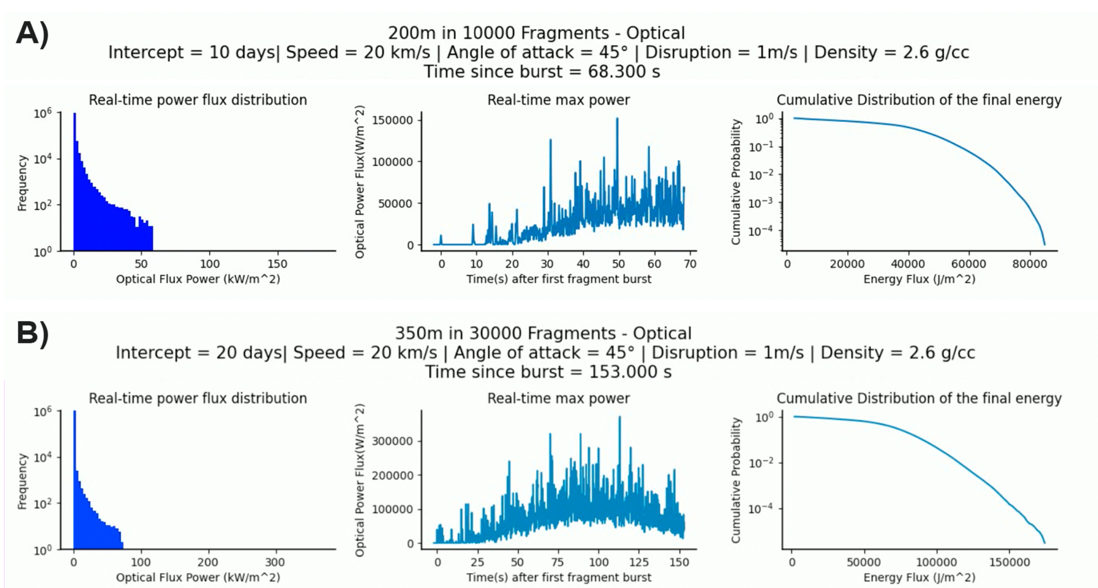

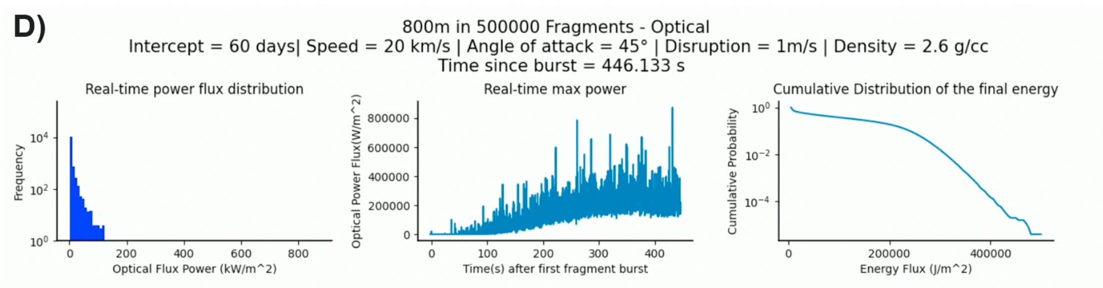

Figure 7. Statistical plots of optical pulse simulations showing mitigation of various potential threats from 200m-800m. Note that each set of plots (A-D) matches the threat cases shown in Figure 6. The left plot shows a histogram distribution of the real-time optical power flux throughout the area; the real-time of each simulation is seen in the title as "Time since burst" (units of sec), dictating the amount of time that has passed since the first airburst of the first fragment. The middle plot shows the real-time maximum optical power throughout the area. The right plot shows the cumulative distribution function (CDF) dictating the frequency of occurrence of various energy flux values.

Acknowledgments

We gratefully acknowledge funding from NASA grant 80NSSC22K0764, NASA California Space Grant NNX10AT93H and funding from the Emmett and Gladys W. Technology Fund. The assistance and exceptional effort provided by the UCSB Experimental Cosmology Group and the entirety of the UCSB Physics Department have been invaluable. We would like to thank our dedicated PI team: our UCSB staff and students, NASA Ames collaborator Darrel K. Robertson, LANL collaborator Mark Boslough, Johns Hopkins APL collaborator Angela Stickle, and all others who have provided tremendous support.

Website and additional materials

This paper and additional papers, simulations and visualizations can be found on our website under the Projects area. Data on our high flux laser tests of ablative materials relevant to supersonic atmospheric entry are also on our website. The PI website area will be updated as new materials and simulations are developed. Detailed simulations can be found on our group YouTube channel, updated regularly.

Website – www.deepspace.ucsb.edu

PI project – www.deepspace.ucsb.edu/projects/pi-terminal-planetary-defense

UCSB Deepspace YouTube channel – www.youtube.com/@UCSBDeepspace

P. Lubin on Research Gate – www.researchgate.net/profile/Philip_Lubin

References

[1] O. P. Popova et al., “Chelyabinsk Airburst, Damage Assessment, Meteorite Recovery, and Characterization,” Science, vol. 342, no. 6162, pp. 1069–1073, Nov. 2013, doi: 10.1126/science.1242642.

[2] P. Brown, R. E. Spalding, D. O. ReVelle, E. Tagliaferri, and S. P. Worden, “The flux of

small near-Earth objects colliding with the Earth,” Nature, vol. 420, no. 6913, pp. 294–296, Nov. 2002, doi: 10.1038/nature01238.
[3] R. Binzel et al., "Apophis 2029: Decadal opportunity for the science of planetary defense," Bulletin of the American Astronomical Society, vol. 53, no. 4, May 2021, doi: 10.3847/25c2cfeb.f87e0599.
[4] D. K. Robertson and D. L. Mathias, "Hydrocode simulations of asteroid airbursts and constraints for Tunguska," Icarus, vol. 327, pp. 36-47, July 2019, doi: 10.1016/j.icarus.2018.10.017.
[5] S. R. Chesley, "Potential impact detection for Near-Earth asteroids: The case of 99942 Apophis (2004 MN4)," Proceedings of the International Astronomical Union, no, 229, pp. 215-228, March 2006, doi: 10.1017/S1743921305006769.
[6] T. G. Müller, C. Kiss, P. Scheirich, P. Pravec, L. O’Rourke, E. Vilenius and B. Altieri, "Thermal infrared observations of asteroid (99942) Apophis with Herschel," Astronomy & Astrophysics, vol. 566, June 2014, doi: 10.1051/0004-6361/201423841.
[7] P. Lubin and A. N. Cohen, "Asteroid interception and disruption for terminal planetary defense," Advances in Space Research, vol. 71, no. 3, pp. 1827-1839, Feb. 2023, doi: 10.1016/j.asr.2022.10.018.
[8] P. Lubin, "PI -- Terminal Planetary Defense," arXiv:2110.07559 [astro-ph, physics:physics], January 2022, arXiv: 2110.07559.
[9] S. Glasstone and P. J. Dolan, “The Effects of Nuclear Weapons. Third edition,” Department of Defense, Washington, D.C. (USA); Department of Energy, Washington, D.C. (USA), TID-28061, Jan. 1977. doi: 10.2172/6852629.
[10] BRODE, H. L., "Review of Nuclear Weapons Effects," Annual Review of Nuclear Science, 18,153 (1968).
[11] Boslough, Mark B., and Harris, Alan, Updated Population and Risk Assessment for Airbursts from Near-Earth Objects (NEOs). United States: N. p., 2014. doi:10.1109/AERO.2015.7119288.
[12] Tziperman, E. (n.d.). Hadley cells. Retrieved March 20, 2023, from https://groups.seas.harvard.edu/climate/eli/research/equable/hadley.html
[13] https://www.youtube.com/@UCSBDeepspace